Braz J Phys (2016) 46:70–77
DOI 10.1007/s13538-015-0385-0

CONDENSED MATTER

Upper Bounds on the Critical Temperature of the Ashkin-Teller Model

Jander P. Santos[1] · **F. C. Sá Barreto**[2]

Received: 6 April 2015 / Published online: 25 November 2015

Abstract Starting from correlation identities for the Ashkin-Teller model and using correlation inequalities, we obtain rigorous upper bounds on the critical temperatures. The results were obtained in hexagonal, square, and cubic lattices and improve over effective field type calculations. The rigorous upper bounds results are compared to those obtained by other methods.

Keywords Ashkin-Teller model · Correlation inequalities · Bounds for the critical temperature · Phase diagrams

1 Introduction

The Ashkin-Teller model [1] is a generalization of the Ising model to a four-component system. It may be considered to be two superposed Ising models, which are, respectively, described by variables S_i and σ_i sitting on each of the sites of a lattice. Within each Ising model, there is a two-spin nearest-neighbor interaction J_{ij}, and the different Ising models are coupled by a four-spin interaction K_{ij}. The Hamiltonian can then be written as

$$H = -\sum_{<ij>} J_{ij}(S_i S_j + \sigma_i \sigma_j) - \sum_{<ij>} K_{ij} S_i \sigma_i S_j \sigma_j \qquad (1)$$

where $< ij >$ denote a pair of a nearest-neighbor spins.

This model presents a variety of phases with second-order transitions lines in hexagonal and square lattices, and first- and second-order transitions lines in the cubic lattice. To study these phase transitions lines, we used an identity for the spin correlation functions obtained in ref [2]. With the expansion of identities in the hexagonal, square, and cubic lattices, we obtained equations for two-spin correlation functions identities with the purpose of applying the rigorous inequalities on the higher order correlation functions to obtain phase diagrams for the Ashkin-Teller model. We look for a representation formula for the spin-spin correlation function $\langle \tau_i \tau_l \rangle$ in terms of higher order correlations $\langle \tau_i \tau_j \cdots \tau_k \tau_l \rangle$, where τ designates anyone of the spin variables of the model, $(S, \sigma, S\sigma)$.

Various methods have been used to describe the properties of the Ashkin-Teller model. In two-dimensions, the mean-field approximation (MFA) was used to obtain the phase diagram for the square lattice [3] and also to study the analytical structure of the free-energy functional [4, 5] to obtain the magnetizations, specific heat, and susceptibility. Renormalization group theory (RG) [6, 7], mean-field renormalization group (MFRG) [8, 9], and Monte Carlo methods (MC) [8–10] were used to obtain the phase diagram for the square lattice. The three-dimensional model on a cubic lattice was analyzed by both the series analysis and the MC method and discussed by Ditzian et al. [3]. Arnold and Zhang [11] studied first-order phase transitions in the

✉ Jander P. Santos
jander@ufsj.edu.br

[1] Departamento de Matemática - UFSJ, Caixa Postal 110, 30301-160, São João del-Rei, MG, Brazil

[2] Departamento de Física - UFMG, Caixa Postal 1621, 30161-970, Belo Horizonte, MG, Brazil

context of the history of the early universe. They proposed MC numerical simulations of the Ashkin-Teller model in three dimensions to study the very weakly first-order phase transitions, specific heat, the correlation length, and the susceptibility across the transition. Musial and others [12]–[17] used MC to study the phase diagram for the cubic lattice. They obtained first- and second-order transitions lines, the tricritical points, and a bifurcation point. An effective field theory was presented to study the critical phase diagrams for the model in two- and three-dimensions [2].

The Ashkin-Teller model has been applied in various areas as magnetism and chemical interactions in metallic alloys [18], thermodynamic properties in superconducting cuprates (CuO_2-plaquettes) [19], in elastic response of DNA molecule to external force and torque [20] and phase diagram of selenium adsorbed on the Ni(100) surface [21].

In Section 2, we show the identity for the spin correlation function for the Ashkin-Teller model derived in ref [2]. In the deduction, it was used of the differential operator technique [22] and the van der Waerden relations. In Section 3, we present of the correlation function identities applied in the hexagonal, square, and cubic lattices. In Section 4, we apply those identities to obtain equations that expresses the spin-spin correlation function $\langle\tau_i\tau_l\rangle$ as a sum of higher order spin-spin correlations. Using the generalization of Griffiths inequalities [23, 24] for the Ashkin-Teller model [25], Newman's inequality [26] and Lebowitz inequalities [27] that ensure the inequalities of Griffiths on an antiferromagnetic system, we replace the above-mentioned equations by inequalities of the type $\langle\tau_i\tau_r\rangle \leq \left[\sum_{\{j:|j|\leq k\}}\alpha_j^{(Z)}(T)\right]\langle\tau_j\tau_r\rangle$, with the purpose to obtain the upper bounds on the critical temperatures T_c, using the decay of correlation function obtained by Simon [28]. In Section 5, we present the numerical results for T_c and the phase transition diagrams. The numerical results based on the identities and the rigorous correlation inequalities are compared to those obtained by other methods. In Section 6, we present the conclusions.

2 Correlation Identity

In this section, we present of the spin-spin correlation identities obtained in ref [2] for the variables τ_i, which designates any one of the variables $(S_i, \sigma_i, S_i\sigma_i)$. These identities are formally a generalization of Callen's identity for the Ising model [29].

We define the thermal average $\langle\tau_i\rangle$ by

$$\langle\tau_i\rangle = \frac{\sum_{\{\tau_i\}}\tau_i e^{-\beta H}}{\sum_{\{\tau_i\}}e^{-\beta H}}, \tag{2}$$

where each τ_i is restricted by $\tau_i = \{-1, 1\}$.

From (1) and (2), we have,

$$\langle F(\{\tau\})\tau_i\rangle = \frac{TrF(\{\tau\})\tau_i e^{-\beta H}}{Tre^{-\beta H}}, \tag{3}$$

where τ_i is the variable at site i and $F(\{\tau\})$ is any function of the variable τ different from τ_i. We can write $H = H_i + H'$, where

$$H_i = -S_i\sum_j J_{ij}S_j - \sigma_i\sum_j J_{ij}\sigma_j - \sigma_i S_i\sum_j K_{ij}\sigma_j S_j \tag{4}$$

is the Hamiltonian describing site i and its neighbors j and H' corresponds to the Hamiltonian of the rest of the lattice. The spin variables commute, i.e., $[\tau_i, \tau_j] = 0$ for all i and j. Consequently, $[H_i, H'] = 0$ and $e^{-\beta H} = e^{-\beta(H_i+H')} = e^{-\beta H_i}e^{-\beta H'}$. From (3) and (4) and using the van der Waerden relation $\tau_i^2 = 1$, it is obtained,

$$\begin{aligned}\langle F(\{\tau\})\tau_i\rangle = \langle F(\{\tau\})\prod_j &[\cosh(\beta J_{ij}\nabla_x)\\ &+S_j\sinh(\beta J_{ij}\nabla_x)].[\cosh(\beta J_{ij}\nabla_y)\\ &+\sigma_j\sinh(\beta J_{ij}\nabla_y)]\\ &\times[\cosh(\beta K_{ij}\nabla_z)\\ &+\sigma_j S_j\sinh(\beta K_{ij}\nabla_z)]\rangle.f_{(\tau)}(x,y,z)|_{\{(0,0,0)\}},\end{aligned} \tag{5}$$

where

$$f_{(S)}(x,y,z) = \frac{\tanh(x)+\tanh(y)\tanh(z)}{1+\tanh(x)\tanh(y)\tanh(z)}, \tag{6}$$

$$f_{(\sigma)}(x,y,z) = \frac{\tanh(y)+\tanh(x)\tanh(z)}{1+\tanh(x)\tanh(y)\tanh(z)} \tag{7}$$

and

$$f_{(\sigma S)}(x,y,z) = \frac{\tanh(z)+\tanh(x)\tanh(y)}{1+\tanh(x)\tanh(y)\tanh(z)}. \tag{8}$$

Expanding the r.h.s of (5) and using $\tau_i^2 = 1$, we obtain,

$$\begin{aligned}\langle F(\{\tau\})\tau_i\rangle = \langle F(\{\tau\})\prod_j &\{[\cosh(\beta J_{ij}\nabla_x)\cosh(\beta J_{ij}\nabla_y)\cosh(\beta K_{ij}\nabla_z)\\ &+\sinh(\beta J_{ij}\nabla_x)\sinh(\beta J_{ij}\nabla_y)\sinh(\beta K_{ij}\nabla_z)]\\ &+S_j[\sinh(\beta J_{ij}\nabla_x)\cosh(\beta J_{ij}\nabla_y)\cosh(\beta K_{ij}\nabla_z)\\ &+\cosh(\beta J_{ij}\nabla_x)\sinh(\beta J_{ij}\nabla_y)\sinh(\beta K_{ij}\nabla_z)]\\ &+\sigma_j[\cosh(\beta J_{ij}\nabla_x)\sinh(\beta J_{ij}\nabla_y)\cosh(\beta K_{ij}\nabla_z)\\ &+\sinh(\beta J_{ij}\nabla_x)\cosh(\beta J_{ij}\nabla_y)\sinh(\beta K_{ij}\nabla_z)]\\ &+\sigma_j S_j[\cosh(\beta J_{ij}\nabla_x)\cosh(\beta J_{ij}\nabla_y)\sinh(\beta K_{ij}\nabla_z)\\ &+\sinh(\beta J_{ij}\nabla_x)\sinh(\beta J_{ij}\nabla_y)\cosh(\beta K_{ij}\nabla_z)]\}\rangle\\ &.f_{(\tau)}(x,y,z)|_{\{(0,0,0)\}}.\end{aligned} \tag{9}$$

Equations (5) and (9) are exact and generalize Callen's identity which was obtained for the spin-1/2 Ising model [29]. In the derivation of (5) and (9), the autocorrelations have been taken explicitly through the van der Waerden relations ($\tau_i^2 = 1$). We use this result (9) in the next section to obtain the identities for the $D2-Z3$ hexagonal lattice, $D2-Z4$ square lattice and $D3-Z6$ cubic lattice.

3 Correlation Function Identities Applied in the Hexagonal, Square, and Cubic Lattices

Developing the (9) for the hexagonal, square, and cubic lattices, we obtain equations for the spin-spin correlation functions in which the rhs contains higher order correlation functions. Considering $F(\{\tau\}) = \tau_r$, we have on the lhs of the identities the correlation function of two spins at sites 0 and r, i.e, the correlation function identities for $\langle\sigma_0\sigma_r\rangle$, $\langle S_0 S_r\rangle$, and $\langle S_0\sigma_0 S_r\sigma_r\rangle$. By the symmetry of the model, we consider $\langle\sigma_0\sigma_r\rangle = \langle S_0 S_r\rangle$. The results obtained for these identities are:

3.1 Correlation Function Identities for the Hexagonal Lattice $D2-Z3$

$$\begin{aligned}\langle\sigma_0\sigma_r\rangle = & A_1^{(3)}\sum_{j=1}^{3}\langle\sigma_j\sigma_r\rangle + A_2^{(3)}\langle\sigma_1\sigma_2\sigma_3\sigma_r\rangle \\ & + A_3^{(3)}\sum_{j<l=1}^{3}\langle S_j\sigma_j S_l\sigma_r\rangle \\ & + A_4^{(3)}\sum_{j<l<m}\langle\sigma_j S_l S_m\sigma_r\rangle \\ & + A_5^{(3)}\sum_{j<l}\langle S_j S_l\sigma_1\sigma_2\sigma_3\sigma_r\rangle \end{aligned} \tag{10}$$

and

$$\begin{aligned}\langle S_0\sigma_0 S_r\sigma_r\rangle = & B_1^{(3)}\sum_{j=1}^{3}\langle S_j\sigma_j S_r\sigma_r\rangle \\ & + B_2^{(3)}\sum_{j<l}\langle\sigma_j S_l S_r\sigma_r\rangle \\ & + B_3^{(3)}\sum_{j}\langle S_1 S_2 S_3\sigma_j S_r\sigma_r\rangle \\ & + B_4^{(3)}\sum_{j}\langle\sigma_1\sigma_2\sigma_3 S_j S_r\sigma_r\rangle \\ & + B_5^{(3)}\langle\sigma_1\sigma_2\sigma_3 S_1 S_2 S_3 S_r\sigma_r\rangle , \end{aligned} \tag{11}$$

where the coefficients $A_i^{(3)}$ and $B_i^{(3)}$ are given in ref. [2].

3.2 Correlation Function Identities for the Square Lattice $D2-Z4$

$$\begin{aligned}\langle\sigma_0\sigma_r\rangle = & A_1^{(4)}\sum_{j}\langle\sigma_j\sigma_r\rangle \\ & + A_2^{(4)}\sum_{j<l<m}\langle\sigma_j\sigma_l\sigma_m\sigma_r\rangle \\ & + A_3^{(4)}\sum_{j<l}\langle S_j\sigma_j S_l\sigma_r\rangle \\ & + A_4^{(4)}\sum_{j<l<m}\langle\sigma_j S_l S_m\sigma_r\rangle \\ & + A_5^{(4)}\sum_{j<l<m}\langle\sigma_j S_l\sigma_l S_m\sigma_m\sigma_r\rangle \\ & + A_6^{(4)}\sum_{j<l<m<n}\langle\sigma_j S_l S_m\sigma_m\sigma_n\sigma_r\rangle \\ & + A_7^{(4)}\sum_{j<l<m}\langle S_1 S_2 S_3 S_4\sigma_j\sigma_l\sigma_m\sigma_r\rangle \\ & + A_8^{(4)}\sum_{j}\langle S_1 S_2 S_3 S_4\sigma_j\sigma_r\rangle \end{aligned} \tag{12}$$

and

$$\begin{aligned}\langle S_0\sigma_0 S_r\sigma_r\rangle = & B_1^{(4)}\sum_{j}\langle\sigma_j S_j S_r\sigma_r\rangle \\ & + B_2^{(4)}\sum_{j<l}\langle\sigma_j S_l S_r\sigma_r\rangle \\ & + B_3^{(4)}\sum_{j<l<m}\langle S_j\sigma_j S_l S_m S_r\sigma_r\rangle \\ & + B_4^{(4)}\sum_{j<l<m}\langle S_j\sigma_j\sigma_l\sigma_m S_r\sigma_r\rangle \\ & + B_5^{(4)}\sum_{j<l<m<n}\langle\sigma_j S_l S_m S_n S_r\sigma_r\rangle \\ & + B_6^{(4)}\sum_{j<l<m<n}\langle S_j\sigma_l\sigma_m\sigma_n S_r\sigma_r\rangle \\ & + B_7^{(4)}\sum_{j<l<m<n}\langle S_j\sigma_j S_l\sigma_l S_m\sigma_n S_r\sigma_r\rangle \\ & + B_8^{(4)}\sum_{j<l<m}\langle S_j\sigma_j S_l\sigma_l S_m\sigma_m S_r\sigma_r\rangle , \end{aligned} \tag{13}$$

where the coefficients $A_i^{(4)}$ and $B_i^{(4)}$ are given in ref. [2].

3.3 Correlation Function Identities for the Cubic Lattice $D3-Z6$

$$
\begin{aligned}
\langle\sigma_0\sigma_r\rangle = {} & A_1^{(6)}\sum_j\langle\sigma_j\sigma_r\rangle \\
& + A_2^{(6)}\sum_{j<l<m}\langle\sigma_j\sigma_l\sigma_m\sigma_r\rangle \\
& + A_3^{(6)}\sum_{j<l<m<n<p}\langle\sigma_j\sigma_l\sigma_m\sigma_n\sigma_p\sigma_r\rangle \\
& + A_4^{(6)}\sum_{j<l}\langle S_j\sigma_j S_l\sigma_r\rangle \\
& + A_5^{(6)}\sum_{j<l<m}\langle\sigma_j S_l S_m\sigma_r\rangle \\
& + A_6^{(6)}\sum_{j<l<m}\langle\sigma_j S_l\sigma_l S_m\sigma_m\sigma_r\rangle \\
& + A_7^{(6)}\sum_{j<l<m<n}\langle\sigma_j S_l S_m\sigma_m\sigma_n\sigma_r\rangle \\
& + A_8^{(6)}\sum_{j<l<m<n<p}\langle\sigma_j S_l S_m\sigma_n\sigma_p\sigma_r\rangle \\
& + A_9^{(6)}\sum_{j<\ldots<p}\langle\sigma_j S_l\sigma_l S_m\sigma_m\sigma_n\sigma_p\sigma_r\rangle \\
& + A_{10}^{(6)}\sum_{j<\ldots<q}\langle\sigma_j S_l\sigma_l S_m\sigma_n\sigma_p\sigma_q\sigma_r\rangle \\
& + A_{11}^{(6)}\sum_{j<\ldots<n}\langle S_j\sigma_j S_l S_m S_n\sigma_r\rangle \\
& + A_{12}^{(6)}\sum_{j<\ldots<p}\langle\sigma_j S_l S_m S_n S_p\sigma_r\rangle \\
& + A_{13}^{(6)}\sum_{j<\ldots<p}\langle S_j\sigma_j S_l\sigma_l S_m\sigma_m S_n\sigma_r\rangle \\
& + A_{14}^{(6)}\sum_{j<\ldots<p}\langle\sigma_j S_l\sigma_l S_m\sigma_m S_n S_p\sigma_r\rangle \\
& + A_{15}^{(6)}\sum_{j<\ldots<q}\langle\sigma_j S_l\sigma_l S_m S_n S_p\sigma_q\sigma_r\rangle \\
& + A_{16}^{(6)}\sum_{j<\ldots<p}\langle\sigma_j S_l\sigma_l S_m\sigma_m S_n\sigma_n S_p\sigma_p\sigma_r\rangle \\
& + A_{17}^{(6)}\sum_{j<\ldots<q}\langle\sigma_j S_l\sigma_l S_m\sigma_m S_n\sigma_n S_p\sigma_q\sigma_r\rangle \\
& + A_{18}^{(6)}\sum_j\langle S_1 S_2 S_3 S_4 S_5 S_6\sigma_j\sigma_r\rangle \\
& + A_{19}^{(6)}\sum_{j<l<m}\langle S_1 S_2 S_3 S_4 S_5 S_6\sigma_j\sigma_l\sigma_m S_r\rangle \\
& + A_{20}^{(6)}\sum_{j<\ldots<p}\langle S_1 S_2 S_3 S_4 S_5 S_6\sigma_j\sigma_l\sigma_m\sigma_n\sigma_p\sigma_r\rangle
\end{aligned}
\tag{14}
$$

and

$$
\begin{aligned}
\langle S_0\sigma_0 S_r\sigma_r\rangle = {} & B_1^{(6)}\sum_j\langle S_j\sigma_j S_r\sigma_r\rangle + B_2^{(6)}\sum_{j<l}\langle S_j\sigma_l S_r\sigma_r\rangle \\
& + B_3^{(6)}\sum_{j<l<m}\langle S_j\sigma_j S_l S_m S_r\sigma_r\rangle \\
& + B_4^{(6)}\sum_{j<l<m<n}\langle\sigma_j S_l S_m S_n S_r\sigma_r\rangle \\
& + B_5^{(6)}\sum_{j<l<m}\langle\sigma_j S_j\sigma_l\sigma_m S_r\sigma_r\rangle \\
& + B_6^{(6)}\sum_{j<l<m<n}\langle S_j\sigma_l\sigma_m\sigma_n S_r\sigma_r\rangle \\
& + B_7^{(6)}\sum_{j<l<m}\langle S_j\sigma_j\sigma_l S_l\sigma_m S_m S_r\sigma_r\rangle \\
& + B_8^{(6)}\sum_{j<l<m<n}\langle S_j\sigma_j S_l\sigma_l S_m\sigma_n S_r\sigma_r\rangle \\
& + B_9^{(6)}\sum_{j<l<m<n<p}\langle S_j\sigma_j S_l S_m\sigma_n\sigma_p S_r\sigma_r\rangle \\
& + B_{10}^{(6)}\sum_{j<\ldots<q}\langle\sigma_j S_l\sigma_m S_n\sigma_p S_q S_r\sigma_r\rangle \\
& + B_{11}^{(6)}\sum_{j<\ldots<p}\langle S_j\sigma_j\sigma_l\sigma_m\sigma_n\sigma_p S_r\sigma_r\rangle \\
& + B_{12}^{(6)}\sum_{j<\ldots<q}\langle S_j\sigma_l S_m\sigma_n S_p\sigma_q S_r\sigma_r\rangle \\
& + B_{13}^{(6)}\sum_{j<\ldots<p}\langle S_j\sigma_j S_l S_m S_n S_p S_r\sigma_r\rangle \\
& + B_{14}^{(6)}\sum_{j<\ldots<q}\langle S_l\sigma_j S_m S_n S_p S_q S_r\sigma_r\rangle \\
& + B_{15}^{(6)}\sum_{j<\ldots<p}\langle S_j\sigma_j\sigma_l\sigma_m S_n\sigma_n S_p\sigma_p S_r\sigma_r\rangle \\
& + B_{16}^{(6)}\sum_{j<\ldots<q}\langle S_j\sigma_j S_l\sigma_l S_m\sigma_n\sigma_p\sigma_q S_r\sigma_r\rangle \\
& + B_{17}^{(6)}\sum_{j<\ldots<p}\langle S_j\sigma_j S_l\sigma_l\sigma_m S_m S_n S_p S_r\sigma_r\rangle \\
& + B_{18}^{(6)}\sum_{j<\ldots<q}\langle S_j\sigma_j S_l\sigma_l S_m S_n S_p\sigma_q S_r\sigma_r\rangle \\
& + B_{19}^{(6)}\sum_{j<\ldots<q}\langle S_j\sigma_j S_l\sigma_l S_m\sigma_m S_n\sigma_n S_p\sigma_q S_r\sigma_r\rangle \\
& + B_{20}^{(6)}\sum_{j<\ldots<p}\langle S_j\sigma_j S_l\sigma_l S_m\sigma_m S_n\sigma_n S_p\sigma_p S_r\sigma_r\rangle,
\end{aligned}
\tag{15}
$$

where the coefficients $A_i^{(6)}$ and $B_i^{(6)}$ are given in ref. [2].

4 Application of the Correlation Inequalities

In this section, we apply the rigorous inequalities on the higher order correlation function appearing in the rhs of the exact identities obtained in the previous Sections 3.1–3.3,

in order to obtain the upper bounds on the critical temperatures T_c, by means of the decay of the correlation functions, as described by Simon [28].

In the higher order spin correlation functions with strictly negative coefficients, we used the generalization of Griffiths's inequality [23, 24] for the Ashkin-Teller model [25], i.e., $\langle \prod_i \tau_i \rangle \geq 0$ for Griffiths I and $\left\langle \prod_i \tau_i \prod_j \tau_j \right\rangle \geq \langle \prod_i \tau_i \rangle \left\langle \prod_j \tau_j \right\rangle$ for Griffiths II.

In the higher order spin correlation functions with strictly positive coefficients, we used Newman's inequality [26] $\langle \tau_i F \rangle \leq \sum_j \langle \tau_i \tau_j \rangle \langle \partial F / \partial \tau_j \rangle$, where F is a product of spin variables (τ). Putting the above information together, we may replace the identities (10)–(15) by the inequality

$$\langle \tau_0 \tau_r \rangle \leq \Big[\sum_{\{j:|j|\leq k\}} \alpha_j^{(Z)}(T) \Big] \langle \tau_j \tau_r \rangle, \tag{16}$$

where $\alpha_j^{(Z)}(T)$ represents the coefficients of the spin-spin correlation functions, where Z is the coordination number of the lattice. The expression (16) when iterated leads to the exponential decay of spin-spin correlations [28] whenever $\sum_{\{j:|j|\leq k\}} \alpha_j^{(Z)}(T) < 1$. Defining $\overline{T}_c$, such that,

$$\sum_{\{j:|j|\leq k\}} \alpha_j^{(Z)}(\overline{T}_c) = 1, \tag{17}$$

the critical temperature T_c must satisfy the bound $T_c < \overline{T}_c$.

The above procedure, i.e, the application of the correlation inequalities on the two-spin correlation equations and the use of the decay of the correlation functions, give the rigorous upper bounds on the critical lines of phase transition, denoted by (AP), (PE) (PD) and (BAF), appearing in the phase diagrams in Fig. 1 discussed in Section 5.

The Ashkin-Teller model presents four different phases in the $2D$ lattices, hexagonal ($Z = 3$), and square ($Z = 4$) lattices, all separated by critical lines of second-order phase transitions. In the cubic lattice ($Z = 6$), the model presents phase transitions of first and second order, tricritical points, bifurcation points and a new phase, which does not appear in the $2D$ phase diagrams. This phase appears between the Baxter phase and the paramagnetic phase, where $\langle \sigma \rangle$ or $\langle S \rangle$ is ordered.

The phases shown by the model, described in terms of the magnetizations, are:

Paramagnetic phase ($Para$): $\langle S \rangle = \langle \sigma \rangle = \langle \sigma S \rangle = 0$,
Baxter phase ($Baxter$): $\langle S \rangle \neq 0$, $\langle \sigma \rangle \neq 0$ and $\langle \sigma S \rangle \neq 0$,
$\langle \sigma S \rangle$-phase ($\langle \sigma S \rangle$): $\langle S \rangle = 0$, $\langle \sigma \rangle = 0$ and $\langle \sigma S \rangle \neq 0$,
$\langle \sigma S \rangle_{AF}$-phase ($\langle \sigma S \rangle_{AF}$): $\langle S \rangle = 0$, $\langle \sigma \rangle = 0$ and $\langle \sigma S \rangle_{AF} \neq 0$, and
$\langle \sigma \rangle$-phase ($\langle \sigma \rangle = \langle S \rangle$), only in the cubic lattice : $\langle \sigma \rangle \neq 0$ and $\langle \sigma S \rangle = 0$.

The application of the correlation inequalities on the identities for each phase transition line in the hexagonal, square, and cubic lattices are presented in the following subsections.

4.1 Phase Transition Line (AP)

To determine the phase transition line (AP) that separates the Baxter phase ($Baxter$) and the paramagnetic phase ($Para$) in the hexagonal, square, and cubic lattices, we use Griffiths II in the correlation functions with strictly negative coefficients ($A_i^{(Z)} < 0$) and Newman's inequality in the correlation functions with strictly positive coefficients ($A_i^{(Z)} > 0$), in the (10), (12), and (14). We get,

$$\begin{aligned} \alpha_j^{(3)} = & [A_1^{(3)} + (-|A_2^{(3)}| - |A_3^{(3)}| - |A_4^{(3)}|) \langle \sigma_1 \sigma_2 \rangle \\ & -|A_5^{(3)}| \langle \sigma_1 \sigma_2 \rangle^2]_{\{AP\}}, \end{aligned} \tag{18}$$

$$\begin{aligned} \alpha_j^{(4)} = & [A_1^{(4)} + (-|A_2^{(4)}| - |A_3^{(4)}| - |A_4^{(4)}|) \langle \sigma_1 \sigma_2 \rangle \\ & +(-|A_5^{(4)}| - |A_6^{(4)}| - |A_8^{(4)}|) \langle \sigma_1 \sigma_2 \rangle^2 \\ & -|A_7^{(4)}| \langle \sigma_1 \sigma_2 \rangle^3]_{\{AP\}} \end{aligned} \tag{19}$$

and

$$\begin{aligned} \alpha_j^{(6)} = & [A_1^{(6)} + 5A_3^{(6)} + 2A_7^{(6)} + 3A_8^{(6)} + 3A_9^{(6)} + A_{14}^{(6)} \\ & +3A_{19}^{(6)} + (-|A_2^{(6)}| - |A_4^{(6)}| - |A_5^{(6)}|) \langle \sigma_1 \sigma_2 \rangle \\ & +(-|A_6^{(6)}| - |A_{11}^{(6)}| - |A_{12}^{(6)}|) \langle \sigma_1 \sigma_2 \rangle^2 \\ & +(-|A_{10}^{(6)}| - |A_{15}^{(6)}| - |A_{18}^{(6)}|) \langle \sigma_1 \sigma_2 \rangle^3]_{\{AP\}}. \end{aligned} \tag{20}$$

As mentioned before, by the symmetry of the model, we considered $\langle S_1 S_2 \rangle = \langle \sigma_1 \sigma_2 \rangle$ in the preceding results.

4.2 Phase Transition Line (PE)

The phase transitions lines (PE) separates the phases (Baxter) and ($\langle S\sigma \rangle$) in the hexagonal, square, and cubic lattices. Therefore, the phase transitions occur on the variables σ and S. As no phase transition occurs in the variable $S\sigma$, we consider $S_k \sigma_k = 1$ in (10), (12), and (14), to obtain the phase transitions only for the variables σ and S. Using Griffiths II in the correlation functions with strictly negative coefficients ($A_i^{(Z)} < 0$) and the Newman's inequality in the correlation functions with strictly positive coefficients ($A_i^{(Z)} > 0$), in (10), (12), and (14), we get,

$$\alpha_j^{(3)} = [A_1^{(3)} + A_3^{(3)} + A_5^{(3)} + (-|A_2^{(3)}| - |A_4^{(3)}|) \langle \sigma_1 \sigma_2 \rangle]_{\{PE\}}, \tag{21}$$

$$\alpha_j^{(4)} = [A_1^{(4)} + A_3^{(4)} + A_5^{(4)} + A_7^{(4)} + (-|A_2^{(4)}| - |A_4^{(4)}| - |A_6^{(4)}| - |A_8^{(4)}|)\,\langle\sigma_1\sigma_2\rangle]_{\{PE\}} \quad (22)$$

and

$$\alpha_j^{(6)} = [A_1^{(6)} + 5A_3^{(6)} + A_4^{(6)} + A_6^{(6)} + 2A_7^{(6)} + 3A_8^{(6)} + 3A_9^{(6)} + A_{14}^{(6)} + 3A_{19}^{(6)} + (-|A_2^{(6)}| - |A_5^{(6)}|)\,\langle\sigma_1\sigma_2\rangle + (-|A_{10}^{(6)}| - |A_{11}^{(6)}| - |A_{12}^{(6)}| - |A_{15}^{(6)}|)\,\langle\sigma_1\sigma_2\rangle^2 + (-|A_{18}^{(6)}|)\,\langle\sigma_1\sigma_2\rangle^3]_{\{PE\}}. \quad (23)$$

By the symmetry of the model, we considered $\langle S_1 S_2\rangle = \langle\sigma_1\sigma_2\rangle$ in the preceding results.

4.3 Phase Transition Line (PD)

To determine the phase transition line (PD) that separates the ($\langle S\sigma\rangle$)-phase and the paramagnetic phase ($Para$) in hexagonal, square, and cubic lattices, we use Griffiths II in the correlation functions with strictly negative coefficients ($B_i^{(Z)} < 0$) and the Newman's inequality in the correlation functions with strictly positive coefficients ($B_i^{(Z)} > 0$), in the (11), (13), and (15). We get,

$$\alpha_j^{(3)} = [B_1^{(3)} + (-|B_2^{(3)}| - |B_3^{(3)}| - |B_4^{(3)}|)\,\langle\sigma_1\sigma_2\rangle - |B_5^{(3)}|\,\langle\sigma_1 S_1\sigma_2 S_2\rangle]_{\{PD\}}, \quad (24)$$

$$\alpha_j^{(4)} = [B_1^{(4)} + (-|B_2^{(4)}| - |B_3^{(4)}| - |B_4^{(4)}| - |B_5^{(4)}| - |B_6^{(4)}|)\,\langle\sigma_1\sigma_2\rangle + 2B_7^{(4)} - |B_8^{(4)}|\,\langle\sigma_1 S_1\sigma_2 S_2\rangle]_{\{PD\}} \quad (25)$$

and

$$\alpha_j^{(6)} = [B_1^{(6)} + B_9^{(6)} + B_{11}^{(6)} + B_{13}^{(6)} + 5B_{20}^{(6)} + (-|B_2^{(6)}| - |B_3^{(6)}| - |B_4^{(6)}| - |B_5^{(6)}| - |B_6^{(6)}|)\,\langle\sigma_1\sigma_2\rangle + (-|B_7^{(6)}|)\,\langle\sigma_1 S_1\sigma_2 S_2\rangle + (-|B_{16}^{(6)}| - |B_{18}^{(6)}|)\,\langle\sigma_1\sigma_2\rangle^3]_{\{PD\}}. \quad (26)$$

By the symmetry of the model, we considered $\langle S_1 S_2\rangle = \langle\sigma_1\sigma_2\rangle$ in the preceding results.

4.4 Phase Transition Line (BAF)

The phase transitions lines (BAF) separates the ($\langle S\sigma\rangle_{AF}$)-phase and the paramagnetic phase ($Para$) in the hexagonal, square, and cubic lattice. To study this phase transition line, we used Lebowitz inequalities [27], that ensure Griffiths inequalities on an antiferromagnetic phase, in the correlation functions with strictly negative coefficients ($B_i^{(Z)} < 0$) and Newman's inequality in the correlation functions with strictly positive coefficients ($B_i^{(Z)} > 0$), in the (11), (13), and (15). We get,

$$\alpha_j^{(3)} = [B_{1_{AF}}^{(3)} + (-|B_{2_{AF}}^{(3)}| - |B_{3_{AF}}^{(3)}| - |B_{4_{AF}}^{(3)}|)\,\langle\sigma_1\sigma_2\rangle - |B_{5_{AF}}^{(3)}|\,\langle\sigma_1 S_1\sigma_2 S_2\rangle]_{\{PD\}}, \quad (27)$$

$$\alpha_j^{(4)} = [B_{1_{AF}}^{(4)} + (-|B_{2_{AF}}^{(4)}| - |B_{3_{AF}}^{(4)}| - |B_{4_{AF}}^{(4)}| - |B_{5_{AF}}^{(4)}| - |B_{6_{AF}}^{(4)}|)\,\langle\sigma_1\sigma_2\rangle_{AF} + 2B_{7_{AF}}^{(4)} - |B_{8_{AF}}^{(4)}|\,\langle\sigma_1 S_1\sigma_2 S_2\rangle_{AF}]_{\{BAF\}} \quad (28)$$

and

$$\alpha_j^{(6)} = [B_{1_{AF}}^{(6)} + B_{9_{AF}}^{(6)} + B_{11_{AF}}^{(6)} + B_{13_{AF}}^{(6)} + 5B_{20_{AF}}^{(6)} + (-|B_{2_{AF}}^{(6)}| - |B_{3_{AF}}^{(6)}| - |B_{4_{AF}}^{(6)}| - |B_{5_{AF}}^{(6)}| - |B_{6_{AF}}^{(6)}|)\,\langle\sigma_1\sigma_2\rangle_{AF} + (-|B_{7_{AF}}^{(6)}|)\,\langle\sigma_1 S_1\sigma_2 S_2\rangle_{AF} + (-|B_{16_{AF}}^{(6)}| - |B_{18_{AF}}^{(6)}|)\,\langle\sigma_1\sigma_2\rangle_{AF}^3]_{\{PD\}}. \quad (29)$$

5 Phase Diagram and Numerical Results

The coefficients of the correlation inequalities obtained in Sections 4.1–4.4 contain correlation functions of two spins separated by two lattice parameters ($\langle\tau_1\tau_2\rangle$). The two-spin correlations results were obtained in the Ashkin-Teller one-dimensional model , and they are given by,

$$\langle\sigma_1\sigma_2\rangle_{(1D)} = \frac{(e^{(4K_2+2K_4)} - e^{2K_4})^2}{(e^{2K_4} + 2\,e^{2K_2} + e^{(4K_2+2K_4)})^2} \quad (30)$$

and

$$\langle S_1\sigma_1 S_2\sigma_2\rangle_{(1D)} = \frac{(e^{2K_4} - 2\,e^{2K_2} + e^{(4K_2+2K_4)})^2}{(e^{2K_4} + 2\,e^{2K_2} + e^{(4K_2+2K_4)})^2} \quad (31)$$

We substitute $\langle\tau_1\tau_2\rangle$=$\langle\tau_1\tau_2\rangle_{(1D)}$ in the coefficients presented in Sections 4.1–4.4. Using condition $\sum_{\{j:|j|\le k\}}\alpha_j^{(Z)}(T) < 1$, we obtain the exponential decay of the correlation function. Therefore, with the (17), we get the rigorous upper bound on the critical temperature $T_c < \overline{T}_c$.

In Fig. 1, we present the phase diagrams of the model for the hexagonal ($D2-Z3$) and square ($D2-Z4$) lattices. Each diagram presents four different phases separated by critical lines of second-order phase transitions (AP), (PE), (PD), and (BAF). The phase transitions were studied as a function of ($K_2 = \beta J$) and ($K_4 = \beta K$). The critical points are designated by the pair (K_4, K_2), which will be presented with four significant digits for a good precision (the four digits comes out of the calculations). The points representing the Ising limit ($K_4 = 0$), the Potts limit ($K_4 = K_2$), and the ($K_4 \to \infty$)-limit are designated by the notation: $C_{Is}^{(Z)}$,

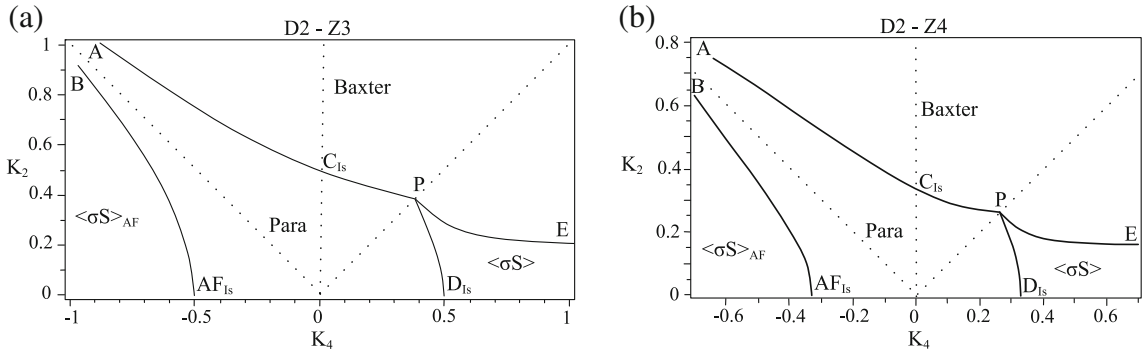

Fig. 1 Phase diagram for the model in the hexagonal ($D2-Z3$) and square ($D2-Z4$) lattices. The Ising limit ($K_4=0$) or ($K_2=0$), the Potts limit ($K_4=K_2$), and the ($K_4\to\infty$)-limit are designated by the notation: C, D, and AF for the Ising limit; P for the Potts limit and E for the ($K_4\to\infty$)-limit. Those points, given by the pair of numbers (K_4, K_2), have the following values $C_{Is}^{(3)}=(0,0.5002)$, $D_{Is}^{(3)}=(0.5003,0)$, $AF_{Is}^{(3)}=(-0.5003,0)$, $C_{Is}^{(4)}=(0,0.3371)$, $D_{Is}^{(4)}=(0.3371,0)$, $AF_{Is}^{(4)}=(-0.3371,0)$, $P^{(3)}=(0.3877,0.3877)$, $P^{(4)}=(0.2736,0.2736)$, $E^{(3)}=(\infty,0.2501)$, and $E^{(4)}=(\infty,0.1658)$, for the hexagonal and square lattices, respectively

$D_{Is}^{(Z)}$, and $AF_{Is}^{(Z)}$ for the Ising limit; $P^{(Z)}$ for the Potts limit and $E^{(Z)}$ for the ($K_4\to\infty$)-limit, where Z stands for the coordination number of the lattice.

The phase $\langle\sigma\rangle$ in 3D is limited by a first-order phase transition line. We cannot obtain this transition line using correlation inequalities; so, we do not present the phase diagram for 3D. However, we present the 3D results in Table 1 for the Ising model limit ($K_4=0$ or $K_2=0$), the four-state Potts model limit ($K_2=K_4$) and the ($K_4\to\infty$) limit. In the paper [2], we studied the effective field and in that case it is possible to obtain the phase $\langle\sigma\rangle$ and lines of first-order transition.

The separation of the ordered phases for the hexagonal ($D2-Z3$), square ($D2-Z4$), and cubic ($D3-Z6$) lattices, are described as follows:

(i) **Baxter phase**: The Baxter phase is limited by two different critical lines of phase transitions, (AP) and (PE), defined by the points A, P, and E . The line (AP) separates the Baxter phase and the paramagnetic phase and the line (PE) separates the Baxter phase and the $\langle\sigma S\rangle$-phase. With $K_4\to 0$, the lines tend to values of K_2 given by $C_{Is}^{(3)}=(0,0.5002)$, $C_{Is}^{(4)}=(0,0.3371)$, and $C_{Is}^{(6)}=(0,0.1833)$ which are the Ising limits. The point P located in the dotted line $K_2=K_4$ coincides with the four-state Potts model, with values $P^{(3)}=(0.3877,0.3877)$, $P^{(4)}=(0.2736,0.2736)$, and $P^{(6)}=(0.1599,0.1599)$. The point A approaches the dotted line $K_2=-K_4$ when $K_4\to-\infty$. The point E tends to half of the value of C_{Is}, i.e., half of the Ising value and it is given

Table 1 Critical temperature T_c obtained by the correlation inequalities (Bounds) and by other methods

	Honeycomb	(D2–Z3)		Square	(D2–Z4)		Cubic	(D3–Z6)	
Points	C_{Is}	P	E	C_{Is}	P	E	C_{Is}	P	E
Exact	0.6584	–	–	0.4407 [30]	0.2746	–	–	–	
Series/MC [3]	–	–	–	–	–	–	0.2168	0.1616	–
MFA [3]	–	–	–	0.25	0.206	–	–	–	–
EFA (Ising) [22]	0.4753	–	–	0.3236		–	0.1971	–	–
CEFA (Ising) [31]	0.5494	–	–	0.4016		–	0.2097	–	–
MFRG [6]	–	–	–	0.346	0.275	–	–	–	–
MFRG [7]	–	–	–	0.3861	–	–	0.2091	0.1701	–
RG [7]	–	–	–	0.4304	0.2795	–	–	–	–
MC [11]	–	–	–	–	–	–	–	0.1571	–
MC [32]	–	–	–	–	–	–	0.2216	–	–
Bounds(Ising) [33]	–	–	–	0.3317	–	–	0.1833	–	–
EFA [2]	0.4753	0.4007	0.2376	0.3236	0.2788	0.1618	0.1971	0.1761	0.0985
Bounds (Present Work)	0.5002	0.3877	0.2501	0.3317	0.2736	0.1658	0.1833	0.1599	0.0916

by $E^{(3)} = (\infty, 0.2376)$, $E^{(4)} = (\infty, 0.1618)$, and $E^{(6)} = (\infty, 0.0916)$.

(ii) $\langle \sigma S \rangle$**-phase**: The critical line PD limits the phase $\langle \sigma S \rangle$ and the paramagnetic phase with point P coinciding with four-state Potts model. In 3D, the point P is different from the bifurcation point that the model presents between the critical lines of phase transitions (PE) and (PD), see ref. [2]. In the limit $K_2 \to 0$, the curves tend to the Ising limits $D_{Is}^{(3)} = (0.5003, 0)$, $D_{Is}^{(4)} = (0.3371, 0)$, and $D_{Is}^{(6)} = (0.1833, 0)$.

(iii) $\langle \sigma S \rangle_{AF}$**-phase**: The critical line (BAF) limits the phase $\langle \sigma S \rangle_{AF}$ and the paramagnetic phase in the region where K_4 has negative sign. In the limit $K_4 \to -\infty$ point B tends to the dotted line $K_2 = -K_4$ and with $K_2 \to 0$ the curves tend to the points $AF_{Is}^{(3)} = (-0.5003, 0)$, $AF_{Is}^{(4)} = (-0.3371, 0)$, and $AF_{Is}^{(6)} = (-0.1833, 0)$, which are the Ising limits.

In Table 1, we show the numerical results for T_c obtained by the present method and those obtained by other methods. For this analysis, we consider the values of the Ising model limit ($K_4 = 0$ or $K_2 = 0$), the four-state Potts model limit ($K_2 = K_4$) and the ($K_4 \to \infty$) limit.

The Ising limit of the Ashkin-Teller model shows the same results obtained by the Ising model for square and cubic lattices [33], as it should.

6 Conclusions

The Ashkin-Teller model has a range of phases which depend on the relationship between the coupling J_{ij} of the two independent spin-1/2 Ising variables S and σ and the coupling K_{ij} between the two variables σS. The different phases of this model exhibit second-order phase transitions in the hexagonal and the square lattices and transitions of first- and second-order in the cubic lattice. We used the spin correlation identities for the Ashkin-Teller model, obtained in ref. [2], which are exact in all dimensions and we have made use of rigorous correlation inequalities to obtain the phase diagrams. The coupling constants obtained for those bounds are calculated for $d = 2$ (honeycomb and square lattices) and $d = 3$ (cubic lattice). All lines of phase transitions obtained by this work are consistent with results obtained by other methods. The importance of the present work is due to the fact that it is rigorous. The results were obtained after using rigorous spin correlation inequalities in spin correlation functions identities. For this reason, they provide rigorous upper bounds on the critical temperatures of the model. Moreover, the numerical results for the critical coupling obtained by the present method, which represent the rigorous bounds, are better than the results obtained by approximated methods [2, 3]. Other methods (MFRG, MC, RG and Series) give better numerical results for the critical coupling, although not based on analitical rigorous procedures.

Acknowledgments JPS financial support from FAPEMIG/Brazil (No. 11.607- FAPEMIG/Brazil). FCSB is grateful to CAPES/Brazil (Project 00035115 (PVNS)-Capes/Brazil) for the financial support that made possible his visit to the UFSJ/Brazil.

References

1. J. Ashkin, E. Teller, Phys. Rev. **64**, 178 (1943)
2. J.P. Santos, F.C. Sá Barreto, Physica A **421**, 316 (2015)
3. R.V. Ditzian, R.J. Banavar, G.S. Grest, L.P. Kadanoff, Phys. Rev. B **22**, 2542 (1980)
4. P.L. Cristiano, S. Goulart Rosa Jr., Phys. Lett. **110A**, 44 (1985)
5. P.L. Cristiano, S. Goulart Rosa Jr., Phys. Rev. B **33**, 07 (1986)
6. J.A. Plascak, F.C. Sá Barreto, Physica A **19**, 2195 (1986)
7. P.M.C. Oliveira, F.C. Sá Barreto, J. Stat. Phys. **57**, 53 (1989)
8. P. Pawlicki, G. Musial, G. Kamieniarz, J. Rogiers, Physica A **242**, 281 (1997)
9. N. Benayad, A. Benyoussef, N. Boccara, A.El. Kenz, J. Phys. C **21**, 5747 (1988)
10. G. Kamieniarz, P. Kozlowski, R. Dekeyser. arXiv:cond–mat/9803277v1 (1998)
11. P. Arnold, Y. Zhang, Nucl. Phys. B **501**, 803 (1997)
12. D. Jeziorek-Kniola, G. Musial, L. Debski, J. Rogiers, S. Dylak, Acta Phys. Polo. A **1105**, 121 (2012)
13. G. Musial, L. Debski, G. Kamieniarz, Phys. Rev. B **66**, 012407 (2002)
14. G. Musial, Phys. Status Solidi B **236**, 486 (2003)
15. G. Musial, Phys. Rev. B **69**, 024407 (2004)
16. G. Musial, J. Rogiers, Phys. Status Solidi B **243**, 335 (2006)
17. P. Pawlicki, G. Musial, G. Kamieniarz, J. Rogiers, Physica A **242**, 281 (1997)
18. M. Sluiter, Y. Kawazoe, Sci. Rep. RITU A **40**, 301 (1995)
19. M.S. Gronsleth, T.B. Nilssen, E.K. Dahl, E.B. Stiansen, C.M. Varma, A. Sudbo. arXiv:Cond-Mat/0806.2665v2 (2009)
20. C. Zhe, W. Ping, Z. Ying-Hong, Commun. Theor. Phys. **49**, 525 (2008)
21. P. Bak, P. Kleban, W.N. Unertl, J. Ochab, G. Akinci, N.C. Bartelt, T.L. Einstein, Phys. Rev. Lett. **54**, 14 (1985)
22. R. Honmura, T. Kaneyoshi, J. Phys. C **12**, 3979 (1979)
23. R.B. Griffiths, J. Math. Phys. **8**, 478 (1967)
24. R.B. Griffiths, J. Math. Phys. **8**, 484 (1967)
25. C.T. Lee, J. Math. Phys. **14**, 1871 (1973)
26. C.M. Newman, Z. Wahrscheintichkeitstheorie verw. Gebiete **33**, 75 (1975)
27. J.L. Lebowitz, Phys. Lett. **36A**, 99 (1971)
28. B. Simon, Math. Phys. **77**, 111 (1980)
29. H.B. Callen, Phys. Lett. **4**, 161 (1963)
30. L. Onsager, Phys. Rev. **65**, 117 (1944)
31. G.B. Taggart, Physica A **113**, 535 (1982)
32. C.F. Baillie, R. Gupta, K.A. Hawick, G.S. Pawley, Phys. Rev. B **45**, 10438 (1992)
33. F.C. Sá Barreto, M.L. O'Carroll, J. Phys. A **16**, 1035 (1983)